Comprehensive Quality Control of Brightness Temperature Data Detected by a Microwave Radiometer

Qiang MA *

Ulanqab Meteorological Bureau, Ulanqab 012000, China

Abstract There are abnormal data of brightness temperature detected by a microwave radiometer in daily use. In this paper, based on the statistical analysis of the observation data of MP3000 microwave radiometer in the southern suburb of Beijing, check of extreme values, time consistency inspection, precipitation inspection, consistency discrimination, power spectrum estimation, and other quality control methods were used to evaluate the data of brightness temperature obtained by the microwave radiometer. It was compared with the observation data of a meteorological tower in Xianghe Station. It is found that the profiles of temperature detected by the microwave radiometer after quality control were very close to the observation results of the tower, indicating that the quality control scheme of the microwave radiometer is feasible and effective.

Key words Microwave radiometer; Quality control; Estimation of brightness temperature; Temperature profile

DOI 10.19547/j.issn2152 -3940.2024.06.002

Due to its own error in the measurement process of a microwave radiometer, the measured data of brightness temperature is too large, which makes the inversion results of atmospheric temperature and humidity profiles worse. The measured data of brightness temperature by a microwave radiometer also has a lot of error information, so it is necessary to carry out the quality control of brightness temperature data. By screening and classifying the data of brightness temperature, the quality control of the data before inversion is carried out. In this paper, based on the statistical analysis of the observation data of MP3000 microwave radiometer in the southern suburb of Beijing and previous research results[1-2], a set of evaluation method of brightness temperature obtained by microwave radiometer, including check of extreme values, time consistency inspection, precipitation inspection, consistency discrimination, power spectrum estimation, *etc.*, was proposed.

1 Quality control of brightness temperature

The flow of comprehensive quality control of brightness temperature detected by the microwave radiometer is shown in Fig. 1.

1.1 Check of extreme values According to the principle of atmospheric radiation transmission, all objects in reality will emit electromagnetic waves outward due to the molecular movement inside them, so that the bright temperature in any frequency band is greater than 0. From the statistics of the precipitation channel of a MP3000 microwave radiometer during precipitation, it is found that most values of brightness temperature are less than 300 K, and only some extreme values exceed 300 K (Fig. 2). Therefore, the range of qualified brightness temperature in the quality control scheme is 0 -300 K.

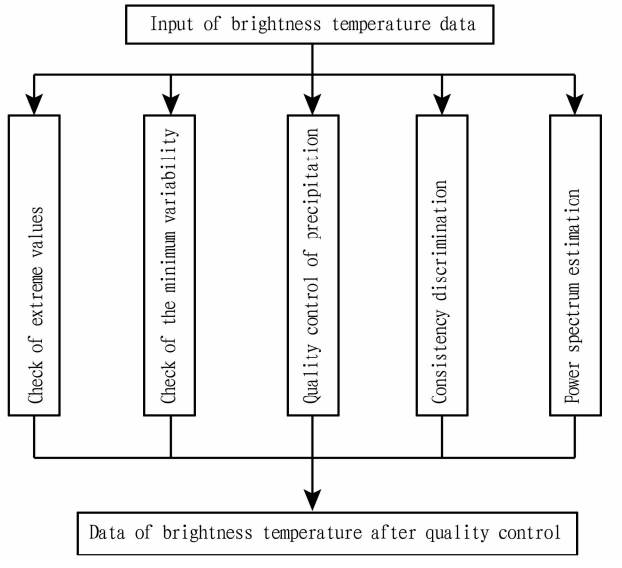

Fig. 1 Flow of comprehensive quality control of brightness temperature detected by the microwave radiometer

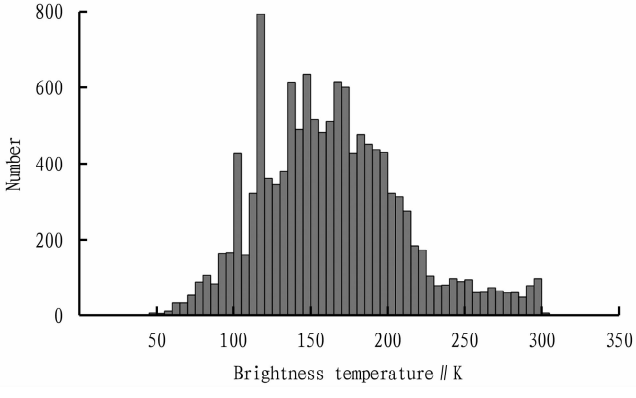

Fig. 2 Statistical histogram of daily brightness temperature measured by MP3000 microwave radiometer during precipitation

Received: November 3, 2024 Accepted: December 6, 2024

* Corresponding author.

1.2 Check of the minimum variability Molecules inside an object are always doing irregular Brownian motion, and the rotation period of the molecules is different; the brightness temperature output by a microwave radiometer is actually the statistical average of brightness temperature, so the values of brightness temperature with high precision in the adjacent periods must be different. After statistics, if the number of adjacent data is 4, the data is inappropriate, and the actual threshold can be set to 5 (Table 1). Fig. 3a shows the changing trend of brightness temperature under normal conditions, and Fig. 3b shows the trend of brightness temperature not changing with continuous time.

Table 1 Frequency of adjacent brightness temperature with the same value

Number of adjacent data	Frequency of the same value
2	1 713
3	808
4	14
5	11

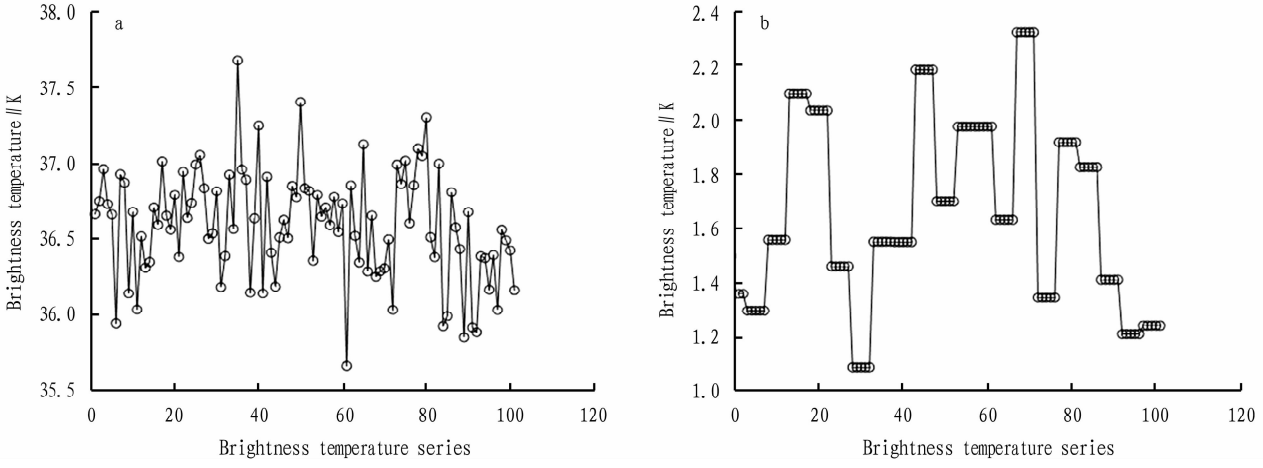

Fig. 3 Changes of normal (a) and abnormal (b) brightness temperature

1.3 Quality control of precipitation During the precipitation process, it can be identified according to its own precipitation sensor. After the precipitation, because the precipitation sensor can not identify it, the water film can be identified by statistical means. Through the statistics of brightness temperature in the non-precipitation period, the precipitation threshold of 120 K can be obtained by taking 97% confidence interval. In addition, since the radiation amount of the water film is much greater than the water vapor radiation in the air, and the reduction of radiation amount of the water film by the continuous evaporation is also much greater than the radiation amplitude of the water vapor in the air during Brownian motion, so the water film can be identified by the continuous decline of brightness temperature. The brightness temperature after quality control in this way may have unidentified abnormal values in adjacent precipitation periods, so it is necessary to conduct another continuity test to obtain a complete elimination of the abnormal brightness temperature of precipitation. The final elimination effect of precipitation quality control is shown in Fig. 4.

1.4 Consistency discrimination From the analysis of the data of brightness temperature in July, it is found that there was more precipitation in summer, and the climate was relatively unstable. During the non-precipitation period (from July 27 to 31), brightness temperature was basically within the 2 K bandwidth channel. When similar atmosphere is studied, it can be extended to the 4 K bandwidth channel. The diagram of probability distribution (Fig. 5) was obtained after the difference of the data of adjacent bright temperature was calculated, and it has high correlation with the fitting curve of the normal distribution. It shows that the Brownian motion of water vapor molecules has general randomness.

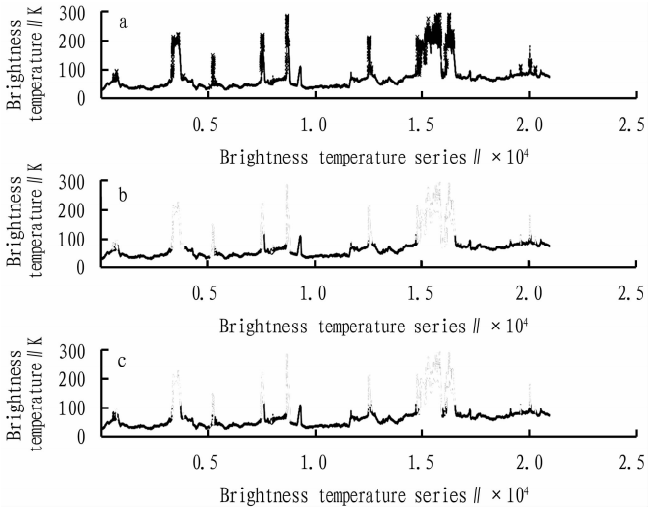

Fig. 4 Original chart of typical brightness temperature in summer (a), chart of precipitation quality control and continuity test (b) and chart of quality control of single precipitation (c)

1.5 Estimation of power spectral density (PSD) The period diagram method was used to analyze the two processes, of which one was stable atmosphere, and the other was strong convective atmosphere. The total time was 10 d, and the period was set to 1 d.

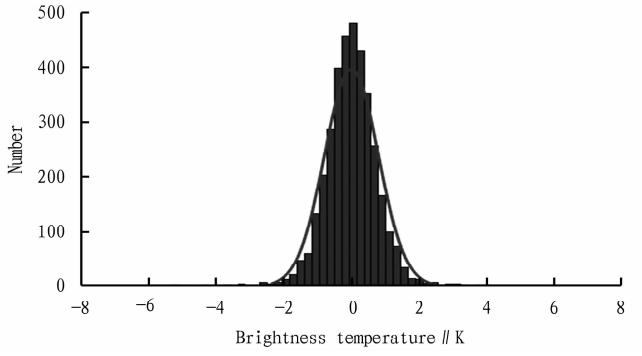

Fig. 5 Distribution of brightness temperature probability

The diagram of frequency domain was obtained after fast Fourier transform (FFT) of time series of brightness temperature was performed (Fig. 6). As can be seen from Fig. 6, the noise was between −25 and −10 dB under clear sky conditions, with the linear fitting slope of −6.8, and the noise signal was relatively stable. Under precipitation conditions, the signal intensity significantly increased, and the noise was between 0 and 20 dB, with the linear fitting slope of −29. The noise smoothness was weaker than the PSD estimation value of bright temperature under clear sky conditions, showing that the unstable factor of the atmosphere was stronger than that under clear sky conditions.

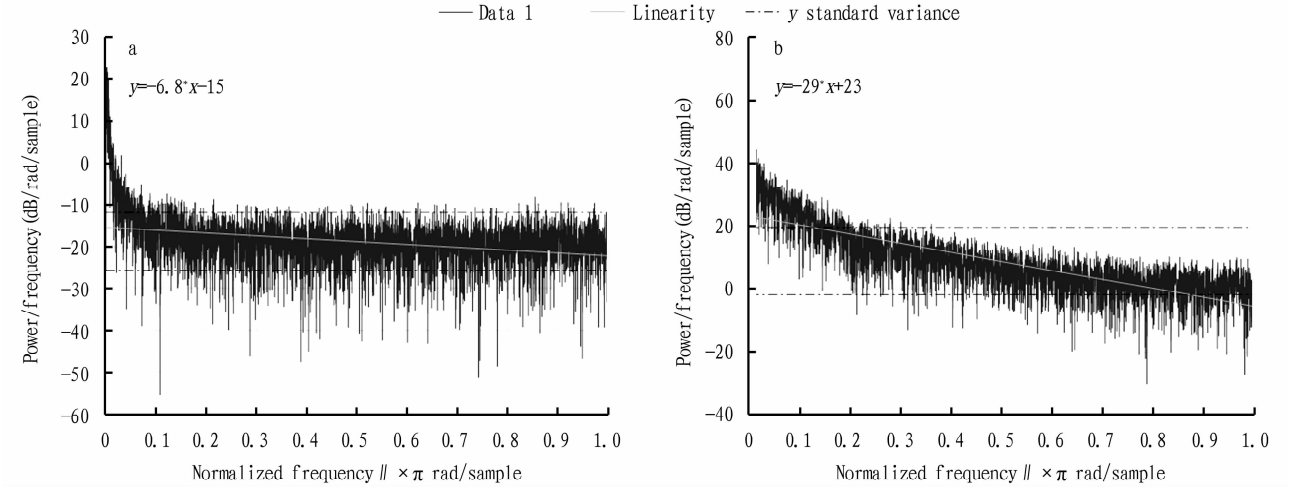

Fig. 6 PSD estimation of bright temperature under clear sky and precipitation conditions

2 Comparison between the data after quality control and actual data

In this paper, the observation data of two individual cases during June 8 − 9 and July 11 − 15 were analyzed, and the temperature and humidity observed by the sounding tower of Beijing Station and the 102-meter meteorological tower of Xianghe Station were compared. From Fig. 7, it can be seen that at 08:00, 10:00 and 14:00 on June 8, there was no rain. The temperature (T) profiles retrieved by the microwave radiometer were very close to the observation results of the tower, and they basically coincided especially at 10:00. There was a certain difference in relative humidity (RH). The distance between the tower and the microwave

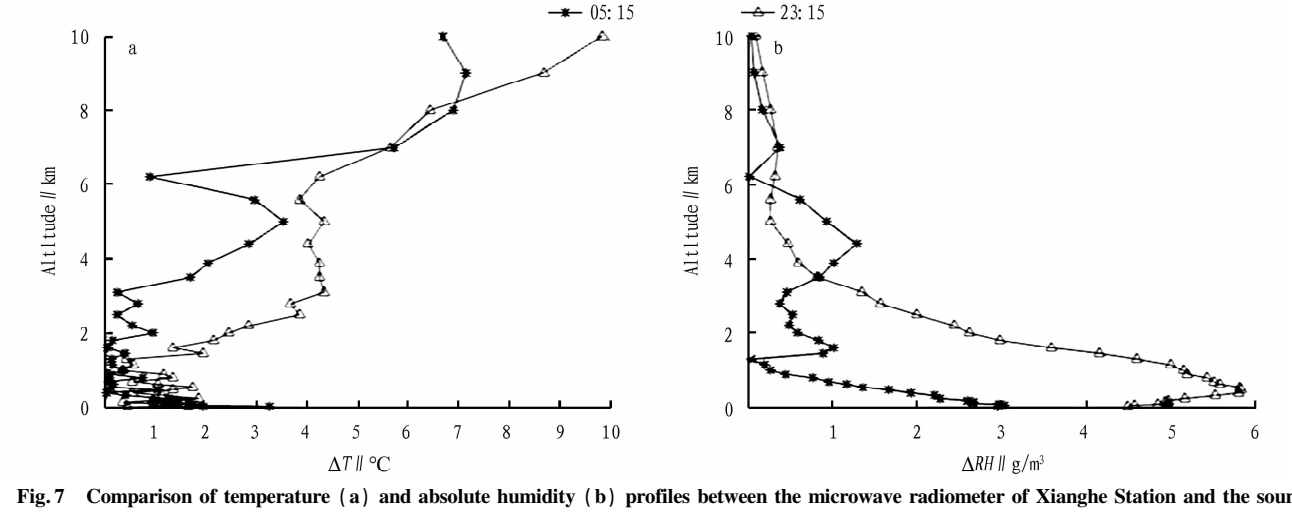

Fig. 7 Comparison of temperature (a) and absolute humidity (b) profiles between the microwave radiometer of Xianghe Station and the sounding tower of Beijing Station on June 8, 2018

(To page 16)

tion of transitional ecological space was the highest, up to 47.83%. The area of core ecological space was 692.86 km^2, accounting for only 10.52%, and it was the smallest among the four types of ecological space. In the core ecological space, the proportion of the area of waters and woodland was large, while the proportion of buildings was the lowest. There was a certain conflict between building land and ecological space, and the proportion of building land was high, which would have a certain impact on the protection of ecological security. The results of this study show that the ecological situation in Nanjing was relatively good. Building land was mainly concentrated in the auxiliary and transitional ecological space. Strictly controlling the urban development boundary (namely limiting the expansion of the city into the scope of ecological space) and increasing the area of artificial green space (such as parks and green belts) in cities and towns can effectively reduce the proportion of construction land in ecological spaces and then the impact on ecological security and protect the ecological environment.

References

[1] WU Q, YANG W, ZHANG LM, *et al.* Study on ecological space protection of Xinyu based on functionality-sensitivity[J]. Guangxi Forestry Science, 2024, 53(5): 658 – 663.

[2] WANG XR, ZOU QY, SHI XY, *et al.* Demarcation of ecological space in Zunhua City based on ecosystem service function and ecological sensitivity [J]. Journal of Shanxi University (Natural Science Edition), 2022, 45 (1): 247 – 256.

[3] GONG WX. Analysis and evaluation of forest ecological status in Ganhe Forestry Bureau[J]. Inner Mongolia Forestry Investigation and Design, 2022, 45(2): 18 – 20.

[4] LI HF. Experiment and analysis of the inversion result of NDVI and RVI based on Landsat[J]. Geospatial Information, 2021, 19(7): 75 – 77.

[5] MA YH, ZHAO MD, ZHOU P, *et al.* Comparison of impervious surface extraction index based on two kinds of satellite sensors[J]. Spacecraft Recovery & Remote Sensing, 2021, 42(2): 139 – 151.

[6] XIONG K, CHANG YP, GUAN J. Monitoring of water area changes based on the normalized difference water index[J]. Central South Forest Inventory and Planning, 2024, 43(2): 54 – 57.

[7] WAN J, WU F, HE YB, *et al.* Clustering algorithm for high-dimensional data under new dimensionality reduction criteria[J]. Journal of Frontiers of Computer Science and Technology, 2020, 14(1): 96 – 107.

[8] ZHAO CL, HU SR. Research on the renewal of public space in small cities based on layer-cake model: A case of the old town of Dayu in Ganzhou, Jiangxi[J]. Urbanism and Architecture, 2022, 19(21): 50 – 56.

(From page 9)

radiometer was 300 m, and the spatial and temporal variation of water vapor was the most significant within 100 m near the ground, so there was a certain difference. At the three moments on June 9, there was rain. It can be seen that there was a significant difference between the temperature profiles of the two, and it reached 10 – 15 K. The values of RH were very close, so it was close to 100%. In the rainfall process from July 11 to 15, similar differences also appeared. That is, before the rainfall, the difference between the two in temperature was small, and there was a certain difference in RH. During the rainfall, the difference in temperature was significant, and atmospheric vapour was almost saturated. As shown in Fig. 9, the average temperature detected by the microwave radiometer was 2.5 ℃ lower than that of the tower when there was no rain, and the mean square error was 1.2 ℃. As there was rain, it was 10.8 ℃ lower, and the mean square error was 4.1 ℃.

3 Conclusions

Based on the measurement principle of bright temperature by microwave radiometer, a set of quality control process of bright temperature data was proposed, in which the effect of water film on the microwave radiometer was corrected. Through the analysis of data at Xianghe Station, the temperature and humidity profiles of the microwave radiometer after quality control was consistent with the data obtained by the 102-meter observation tower when there was no rain.

References

[1] MAO JJ, JIAO ZM, ZHANG XF, *et al.* Influence analysis of hydrophobic layer aging of radome on microwave radiometer observation[J]. Meteorological Science and Technology, 2022, 50(6): 759 – 765.

[2] FU XS, TAN JG. Quality control of temperature and humidity profile retrievals from ground-based microwave radiometer[J]. Journal of Applied Meteorological Science, 2017, 28(2): 202 – 217.